Note

Discovery and Synthesis of a Novel Series of Liver X Receptor Antagonists

Siyun Nian,[a] Xia Gan,[a] Xiangduan Tan,[b] Zhenpeng Yu,[c] Panfeng Wang,[c] Xing Chen,[a] and Guoping Wang*[,a,c]

[a] *Shanghai Institute of Pharmaceutical Industry, China State Institute of Pharmaceutical Industry; Shanghai 200437, P.R. China:* [b] *College of Pharmacy, Guilin Medical University; Guilin, Guangxi 541004, P.R. China: and* [c] *Shanghai Shyndec Pharmaceutical Co., Ltd.; Shanghai 200437, P.R. China.*

Received March 21, 2015; accepted May 17, 2015; advance publication released online June 11, 2015

Fourteen novel compounds were prepared and their antagonistic activities against liver X receptors (LXR) α/β were tested *in vitro*. Compound 26 had an IC_{50} value of 6.4 μM against LXRα and an IC_{50} value of 5.6 μM against LXRβ. Docking studies and the results of structure–activity relationships support the further development of this chemical series as LXRα/β antagonists.

Key words liver X receptor α; liver X receptor β; antagonistic activity

Nuclear receptors (NRs) are ligand-activated transcription factors that coordinate gene expression in response to the modulation of metabolism, development, proliferation, and inflammation.[1,2] Liver X receptors (LXRs) belonging to the NR superfamily are activated by specific oxidized forms of cholesterol and intermediate products of the cholesterol biosynthetic pathway.[1,3,4] There are two LXR isoforms in mammals, termed LXRα and LXRβ. LXRα is abundantly expressed mainly in the liver, intestine, kidney, spleen, and adipose tissue, whereas LXRβ is more ubiquitously expressed, with particularly high levels in the developing brain.[5–8] Both isoforms share almost 80% homology of their amino acid sequences in their DNA-binding domain and ligand-binding domain.[5,7]

The LXR consists of four domains: N-terminal ligand-independent activation function domain (AF-1); DNA-binding domain (DBD); hydrophobic ligand-binding domain (LBD); and C-terminal ligand-dependent transactivation sequence (AF-2).[5,9,10] By forming heterodimers with retinoid X receptors (RXRs), LXRs bind to LXR response elements (LXREs) in the promoter or enhancer elements of LXR target genes. The activation of LXR-RXR heterodimers not only induces the expression of a variety of target genes (CYP7A, ABCA1, SREBP-1) that are involved in lipid and glucose metabolism, but also results in the inhibition of genes encoding inflammatory factors such as tumor necrosis factor (TNF)-α, interleukin (IL)-1β, and interferon (IFN)-γ.[1,11–15]

In the last decade, GlaxoSmithKline and other several pharmaceutical companies have been active in developing synthetic LXR agonists (Fig. 1). T0901317 (**1**, Tularik) and GW3965 (**2**, GSK) exhibit nonselectivity for LXRα and LXRβ with high affinity.[11,16–18] The first compound to enter the clinic was LXR-623 (**3**, Wyeth), an LXRα/β partial agonist for the potential treatment of atherosclerosis and dyslipidemia. Unfortunately, the trial was terminated due to adverse central nervous system effects.[19–21] LXR antagonists reported so far include riccardin C (**4**, antagonist of LXRβ), naringenin (**5**, antagonist of LXRα), genistein (**6**, inhibition of LXRα or activation of LXRβ), taurine (**7**, antagonist of LXRα), rhein (**8**, antagonist of LXRα/β), SR-9238 (**9**, antagonist of LXRα/β), and **10** (antagonist of LXRα), among others[22–28] (Fig. 1). SR-9238 was the first selective synthetic LXR inverse agonist that displays a degree of LXRβ selectivity with an IC_{50} value of 214 nM for LXRα and 43 nM for LXRβ, and this compound effectively suppressed hepatic lipogenesis, inflammation, and hepatic lipid accumulation in a mouse model of nonalcoholic hepatosteatosis.[27]

In this paper, we describe the discovery and further structural development of LXR antagonists based on the fibrate skeleton. Both molecules activated LXRs in a luciferase reporter gene assay (GAL4) tested in HEK-293 cells.[29] In our previous studies, we first found that the combination of gemfibrozil and 4′-hydroxyacetophenone *via* the amide bond provided compound **15a** (Fig. 2), which exhibited weak antagonistic activity toward LXRα and LXRβ, and then we took ciprofibrate, bezafibrate, and fenofibrate as templates to design **15b**–**d** in the same manner as described for the preparation of **15a**. Finally, the fenofibrate template was combined with substitued acetophenone to obtain further compounds as LXR antagonists.

Results and Discussion

Chemistry Compounds **15a**–**d** were synthesized starting with the preparation of 2-amino-1-(4-hydroxyphenyl)ethanone hydrochloride **13** by Delépine reaction at low temperature, followed by condensation of carboxylic acids **14a**–**d** in the presence of 1-(3-dimethylaminopropyl)-3-ethylcarbodiimide hydrochloride (EDCI·HCl) and 1-hydroxybenzotriazole (HOBT) at room temperature[30,31] (Chart 1). **14a** and **d** were converted into **16a** and **d** in the presence of *N*,*N*′-carbonyldiimidazole (CDI) under an H_2S atmosphere, and then **14a**, **d**, **16a**, and **d** were allowed to react with 2-bromo-4′-hydroxyacetophenone **11** in the presence of K_2CO_3[32,33] (Chart 2). Compounds **22e**–**i** were synthesized as shown in Chart 3, using a route nearly identical to that in Chart 1.[30,31] The amide **24** was prepared by condensation of carboxylic acid **14d** and 1-(*tert*-butoxycarbonyl)piperazine **23** with EDCI·HCl as a condensation agent and 4-dimethylaminopyridine (DMAP) as a catalyst in CH_2Cl_2.[34] The deprotection of the *tert*-butoxycarbonyl (Boc) group on the amino group by hydrolysis with trifluoroacetic acid (TFA) was carried out at room temperature, then

* To whom correspondence should be addressed. e-mail: wgpsipich@163.com

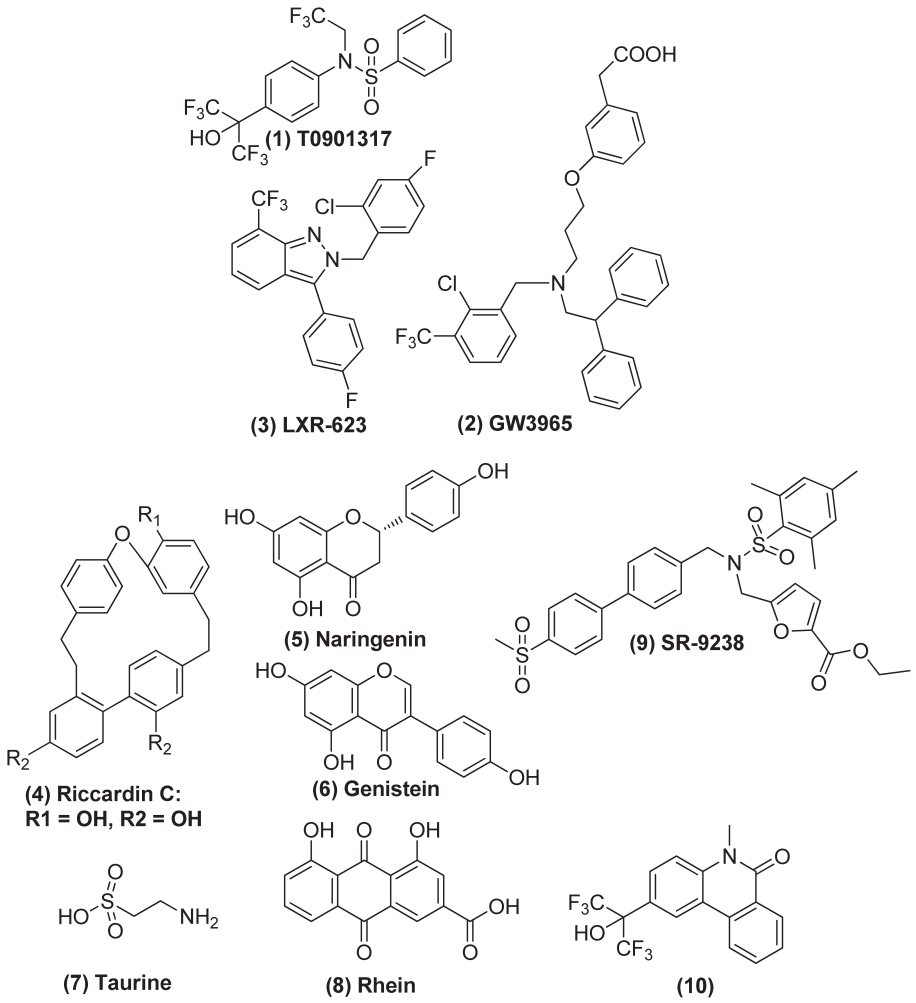

Fig. 1. Chemical Structures of LXR Agonists (**1**–**3**) and LXR Antagonists (**4**–**10**)

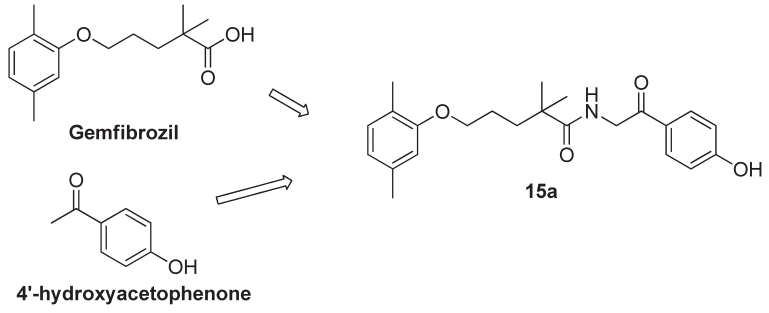

Fig. 2. Design of Compound **15a**

basified to transform into compound **25**, and alkylated with 2-bromo-4′-hydroxyacetophenone **11** under basic conditions to generate compound **26**[35,36] (Chart 4).

Biological Activity As shown in Table 1, under our experimental conditions, the extent of inhibition by **15a** at 25 μM was 35.6% and 26.8% for LXRα and LXRβ, respectively. Surprisingly, **15d** reached inhibition rates of 57.6% and 61.2%, respectively.

Based on the above findings, we tried to improve the antagonistic activity of compounds **15a** and **d** by replacing the amide linker with ester and thioester linkers, resulting in **17a**, **18a**, **17d**, and **18d**. The inhibition rates of these four compounds along with those of **15a**, **d**, gemfibrozil, and fenofibrate are listed in Table 2. Gemfibrozil and fenofibrate exhibited no antagonistic activity against LXRs, but their analogues did. In particular, **15d** showed inhibition rates of 68.0% for LXRα and 65.2% for LXRβ. In the two series of compounds, the inhibition rate for LXRs were in the order: **15a**>**17a**>**18a**, **15d**>**17d**>**18d**, indicating that the amide linker plays a key role in the antagonistic activity. Because the order of potency was **15d**>**a**, **17d**>**a**, and **18d**>**a**, this indicates that the fenofibrate skeleton may enhance the antagonistic activity in our designed compounds.

Taking advantage of the above information, we speculated that condensation products of the core scaffold fenofibrate with other substituted acetophenones *via* the key amide linker

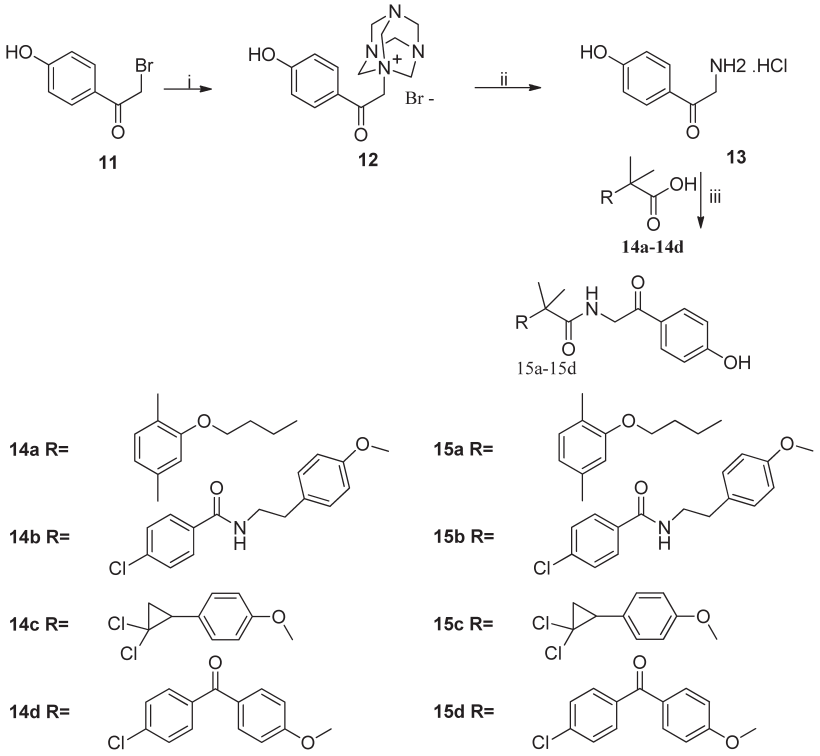

Reagents and conditions: (i) Hexamethylenetetramine, THF, rt; (ii) Conc. HCl, ethanol, 45°C; (iii) HOBT, EDCI·HCl, triethylamine, CH_2Cl_2, rt.

Chart 1. General Route for the Synthesis of **15a**–**d**

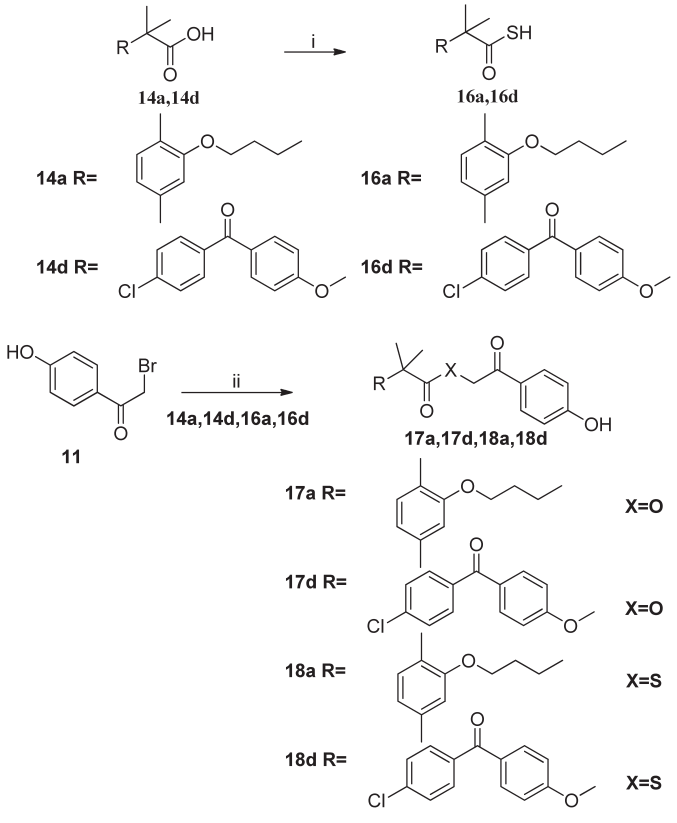

Reagents and conditions: (i) CDI, H_2S, DMF; (ii) K_2CO_3, THF.

Chart 2. General Route for the Synthesis of **17a**, **d**, **18a**, and **d**

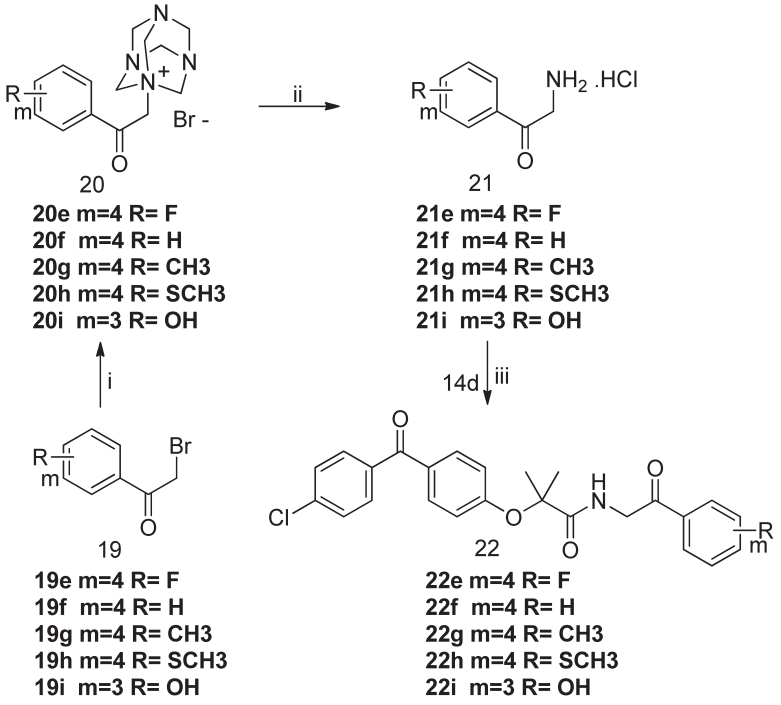

Reagents and conditions: (i) Hexamethylenetetramine, THF, rt; (ii) Conc. HCl, ethanol, 45°C; (iii) HOBT, EDCI·HCl, triethylamine, CH_2Cl_2, rt.

Chart 3. General Route for the Synthesis of **22e**–**i**

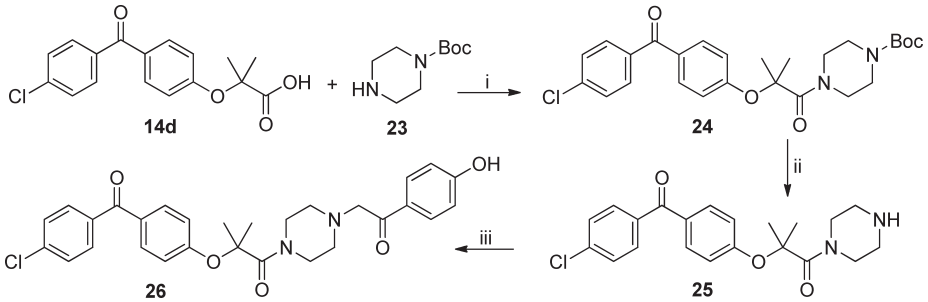

Reagents and conditions: (i) EDCI·HCl, DMAP, triethylamine, CH_2Cl_2; (ii) TFA, THF; (iii) K_2CO_3, THF.

Chart 4. General Route for the Synthesis of Compound **26**

Table 1. Inhibition (%) by **15a**–**d** at 25 μM of LXRs[a)]

Compound	LXRα	LXRβ
15a	35.6±2.7	26.8±6.4
15b	12.9±1.8	8.4±4.9
15c	4.4±4.1	−13.6±1.4
15d	57.6±2.0	61.2±5.1

a) Results are given as the mean±S.D. of two independent experiments.

Table 2. Inhibition (%) by **15a**, **d**, **17a**, **d**, **18a**, **d**, Gemfibrozil, and Fenofibrate at 25 μM of LXRs[a)]

Compound	LXRα	LXRβ
15a	38.9±3.0	30.2±4.2
17a	18.8±1.9	23.6±12.2
18a	0.8±4.5	7.6±5.8
Gemfibrozil	−4.3±9.7	−10.4±10.6
15d	68.0±14.0	65.2±6.7
17d	38.4±5.2	43.4±3.1
18d	17.5±5.7	24.3±7.0
Fenofibrate	−20.7±8.7	−14.8±5.5

a) Results are given as the mean±S.D. of two independent experiments.

might possess potent antagonistic activity against LXRs. Therefore another six compounds were prepared and their antagonistic activities were determined *in vitro* (Table 3), using clotrimazole[37)] as the standard reference. With a longer chain, compound **26** had an IC_{50} value of 6.4 μM for LXRα and 5.6 μM for LXRβ, which was two-fold more potent than **15d**, while compound **22g** had an IC_{50} value of 30.6 μM for LXRα and 19.2 μM for LXRβ. Compounds **22e**, **f**, **h**, and **i** also showed good antagonistic activity, although not as effective as **15d**. The structure–activity relationship (SAR) indicating the extension of the amide linker for this class may enhance the antagonistic activity against LXRs.

Molecular Docking The predicted interaction between the protein and ligand is shown in Fig. 3. For LXRα, the phenolic hydroxyl group formed a strong hydrogen bond with His421, and the substituted phenolic hydroxyl group is seen as a hydrogen bond to Thr302. The left-hand side phenolic

hydroxyl phenyl ring is embedded in a hydrophobic pocket formed by Leu331, Phe335, and Leu428, while the right-hand side chlorine-substituted phenyl ring is inserted into a hydrophobic pocket formed by Leu260, Ser264, Phe315, and Leu316. Also, a pair of π–π interactions exists between the middle phenyl ring and Phe315. For LXRβ, the phenolic hydroxyl group formed a strong hydrogen bond with Ala343, while the left-hand side phenolic hydroxyl phenyl ring occupied a hydrophobic pocket formed by Phe268, Leu345, and Leu442, and the right-hand side conjugated phenyl ring was embedded in a hydrophobic pocket formed by Ser278, Met312, Thr316, Phe329, and Leu330.

Conclusion

In summary, we synthesized 14 novel compounds that exhibited different antagonistic activitives against LXRα/β. Among these compounds, compound **26** had antagonistic activity two-fold more potent than **15d** toward LXRα/β and its binding was predicted. SAR studies indicated that compounds with the amide linker were more potent than compounds with ester and thioester linkers. Furthermore, a longer chain between the fenofibrate template and the acetophenone template may enhance the antagonistic activity. Further research is required to optimize this scaffold for the design of more potent LXRα/β antagonists.

Experimental

Chemistry Melting points were determined on a WRS-21 melting point apparatus (Shanghai Shen Guang Instrument Co., Ltd., Shanghai, P.R. China) and were uncorrected.

Table 3. IC_{50} Values (μM) of **15d**, **22e–i**, and **26** against LXRs[a)]

Compound	LXRα	LXRβ
15d	12.2	12.7
22e	16.9	14.8
22f	15.9	16.2
22g	30.6	19.2
22h	16.1	15.2
22i	13.2	17.6
26	6.4	5.6
Clotrimazole[b)]	10.1	11.8

a) Results are given as the mean of two independent experiments. *b*) Standard reference.

^{1}H-NMR spectra were recorded on an INOVA 400 (400-MHz) spectrometer (Varian Inc., Palo Alto, CA, U.S.A.) with tetramethylsilane (TMS) as an internal standard. Chemical shifts (δ) are in ppm relative to TMS, and coupling constants (J) are expressed in hertz (Hz). Electron-spray ionization mass spectra (ESI-MS) in positive mode were recorded on a HP5989A mass spectrometer (Hewlett-Packard, Palo Alto, CA, U.S.A.). The purity of all novel compounds was checked using TLC and ^{1}H-NMR. All reactions were monitored using TLC on precoated Silica Gel F254 plates (Yantai Jiang You Silicone Development Co., Ltd., Yantai, P.R. China) with detection by UV. All reagents used were of analytical grade (J&K Scientific Ltd., Beijing, P.R. China, Aladdin Industrial Inc., Shanghai, P.R. China, or Sinopharm Chemical Reagent Co., Ltd., Beijing, P.R. China).

General Procedure for the Synthesis of 15a–d[30,31] To a solution of 2-bromo-4′-hydroxyacetophenone **11** (20.0 mmol) in tetrahydrofuran (THF) (50 mL), hexamethylenetetramine (20.0 mmol) was added and stirred for 3 h at room temperature, and then the precipitated hexamethylenetetramine adduct **12** was filtered out. The adduct **12** was then heated with ethanol (80 mL) and concentrated HCl (8 mL) for 1 h at 45°C. After cooling, the inorganics were filtered out, the mixture was washed with ethanol (20 mL), and the solvent was distilled out completely under reduced pressure to obtain the desired compound **13**. Then **14a–d** (2.0 mmol), triethylamine (4.0 mmol), and EDCI·HCl (4.0 mmol), followed by HOBT (4.0 mmol), were added to a stirred solution of **13** (2.0 mmol) in CH_2Cl_2 (10 mL) and the mixture was stirred for 12 h at room temperature. Saturated Na_2CO_3 was added, the mixture was extracted with ethyl acetate, and the extracts were washed with brine, dried over $MgSO_4$, filtered, and concentrated. The residue was purified by chromatography to give target compounds **15a–d**.

5-(2,5-Dimethylphenoxy)-*N*-(2-(4-hydroxyphenyl)-2-oxoethyl)-2,2-dimethylpentanamide (**15a**): Yield 75%, mp 131.2–134.3°C. ^{1}H-NMR (400 MHz, $CDCl_3$) δ: 1.16 (6H, s), 1.62–1.73 (4H, m), 2.10 (3H, s), 2.25 (3H, s), 3.89–3.92 (2H, m), 4.44–4.46 (2H, d, J=5.6 Hz), 6.61–6.63 (1H, d, J=8.0 Hz), 6.71 (1H, s), 6.85–6.99 (2H, m), 7.67–7.69 (1H, m), 7.85–7.88 (2H, m), 10.30 (1H, s). ESI-MS *m/z*: 384 $[M+H]^+$.

4-Chloro-*N*-(4-((1-((2-(4-hydroxyphenyl)-2-oxoethyl)amino)-2-methyl-1-oxopropan-2-yl)oxy)phenethyl)benzamide (**15b**): Yield 74%, mp 216.0–220.4°C. ^{1}H-NMR (400 MHz, $CDCl_3$) δ: 1.38 (6H, s), 2.73–2.76 (2H, m), 3.47–3.48 (2H, m), 4.55–4.56 (2H,

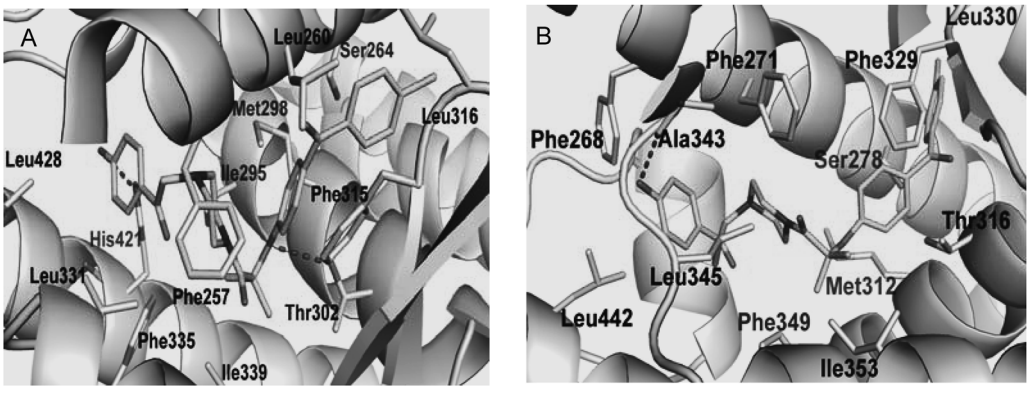

Fig. 3. Binding Modes of **26** to LXRα and LXRβ

(A) Binding mode of **26** within the LXRα-LBD; (B) Binding mode of **26** within the LXRβ-LBD. The ligand is depicted as sticks, amino acids involved in ligand binding are shown as gray sticks, and hydrogen bonds are denoted by dotted lines.

d, J=4.8 Hz), 6.75–6.81 (4H, m), 6.99–7.01 (2H, d, J=8.0 Hz), 7.16 (1H, s), 7.21–7.23 (2H, d, J=8.8 Hz), 7.21 (1H, s), 7.58–7.61 (2H, d, J=8.4 Hz), 7.63 (1H, s), 7.70–7.72 (2H, d, J=8.8 Hz). ESI-MS m/z: 495 $[M+H]^+$.

2-(4-(2,2-Dichlorocyclopropyl)phenoxy)-*N*-(2-(4-hydroxyphenyl)-2-oxoethyl)-2-methylpropanamide (**15c**): Yield 72%, mp 113.6–115.9°C. ^{1}H-NMR (400 MHz, $CDCl_3$) δ: 1.55 (6H, s), 1.93–1.97 (2H, m), 2.82–2.88 (1H, m), 4.71–4.72 (2H, d, J=4.8 Hz), 6.89–6.99 (4H, m), 7.15–7.16 (2H, d, J=5.2 Hz), 7.72 (1H, s), 7.88–7.90 (2H, d, J=8.8 Hz). ESI-MS m/z: 422 $[M+H]^+$.

2-(4-(4-Chlorobenzoyl)phenoxy)-*N*-(2-(4-hydroxyphenyl)-2-oxoethyl)-2-methylpropanamide (**15d**): Yield 65%, mp 172.4–174.3°C. ^{1}H-NMR (400 MHz, $CDCl_3$) δ: 1.67 (6H, s), 4.70–4.71 (2H, d, J=4.8 Hz), 6.64 (1H, s), 6.91–6.93 (2H, d, J=8.8 Hz), 7.05–7.07 (2H, m), 7.45–7.47 (2H, d, J=8.4 Hz), 7.61 (1H, s), 7.71–7.83 (6H, m). ESI-MS m/z: 452 $[M+H]^+$.

General Procedure for the Synthesis of 17a, d, 18a, and d[32,33] CDI (10.0 mmol) was dissolved in *N*,*N*-dimethylformamide (DMF) (20 mL) and to this solution a solution of the carboxylic acids **14a** and **d** (10.0 mmol) in DMF (2 mL) was added dropwise. Subsequently, the reaction mixture was stirred at room temperature for 1 h. Then, H_2S was bubbled gently through the reaction mixture for 2 h. Sulfuric acid (0.5 M, 40 mL) was added and the mixture was extracted with ethyl acetate. The organic layer was dried with magnesium sulfate ($MgSO_4$), filtered, and concentrated to yield **16a**, **d**, **14a**, **d**, **16a**, and **d** (2.0 mmol). They were dissolved in THF (10 mL), anhydrous K_2CO_3 (4.0 mmol) and 2-bromo-4′-hydroxyacetophenone **11** (2.0 mmol) were added, and the mixture was stirred for 4 h at room temperature. Dilute HCl was added, and the mixture was extracted with ethyl acetate, washed with brine, dried over $MgSO_4$, filtered, and concentrated, and the residue was purified by chromatography to afford target compounds **17a**, **d**, **18a**, and **d**.

2-(4-Hydroxyphenyl)-2-oxoethyl-5-(2,5-dimethylphenoxy)-2,2-dimethylpentanoate (**17a**): Yield 83%, mp 105.6–108.3°C. ^{1}H-NMR (400 MHz, $CDCl_3$) δ: 1.32 (6H, s), 1.81–1.85 (4H, m), 2.18 (3H, s), 2.30 (3H, s), 3.94–3.97 (2H, m), 5.23 (2H, s), 5.62 (1H, s), 6.63–6.66 (2H, m), 6.85–6.87 (2H, m), 6.98–7.00 (1H, d, J=7.6 Hz), 7.80–7.82 (2H, m). ESI-MS m/z: 385 $[M+H]^+$.

2-(4-Hydroxyphenyl)-2-oxoethyl-2-(4-(4-chlorobenzoyl)-phenoxy)-2-methylpropanoate (**17d**): Yield 89%, mp 112.0–115.2°C. ^{1}H-NMR (400 MHz, $CDCl_3$) δ: 1.79 (6H, s), 5.35 (2H, s), 6.21 (1H, s), 6.87–6.88 (2H, m), 7.02–7.26 (2H, m), 7.44–7.46 (2H, d, J=8.8 Hz), 7.70–7.81 (6H, m). ESI-MS m/z: 453 $[M+H]^+$.

S-(2-(4-Hydroxyphenyl)-2-oxoethyl)-5-(2,5-dimethylphenoxy)-2,2-dimethylpentanethioate (**18a**): Yield 67%, mp 90.3–93.9°C. ^{1}H-NMR (400 MHz, $CDCl_3$) δ: 1.32 (6H, s), 1.84–1.86 (4H, m), 2.18 (3H, s), 2.30 (3H, s), 3.94–3.97 (2H, m), 5.24 (2H, s), 5.68 (1H, s), 6.63–6.66 (2H, m), 6.86–6.88 (2H, m), 6.99–7.01 (1H, d, J=7.2 Hz), 7.80–7.82 (2H, m). ESI-MS m/z: 423 $[M+Na]^+$.

S-(2-(4-Hydroxyphenyl)-2-oxoethyl)-2-(4-(4-chlorobenzoyl)-phenoxy)-2-methylpropanethioate (**18d**): Yield 57%, mp 150.1–153.6°C. ^{1}H-NMR (400 MHz, $CDCl_3$) δ: 1.65 (6H, s), 4.33 (2H, s), 5.57 (1H, s), 6.88–6.90 (2H, d, J=8.8 Hz), 6.99–7.01 (2H, d, J=8.8 Hz), 7.45–7.47 (2H, d, J=8.4 Hz), 7.71–7.74 (2H, m), 7.91–7.93 (2H, d,=8.4 Hz). ESI-MS m/z: 491 $[M+Na]^+$.

General Procedure for the Synthesis of 22e–i[30,31] Compounds **22e**–**i** were prepared from **19e**–**i** by means of a procedure similar to that used for **15a**–**d**.

2-(4-(4-Chlorobenzoyl)phenoxy)-*N*-(2-(4-fluorophenyl)-2-oxoethyl)-2-methylpropanamide (**22e**): Yield 82%, mp 125.8–125.9°C. ^{1}H-NMR (400 MHz, $CDCl_3$) δ: 1.66 (6H, s), 4.75–4.78 (2H, d, J=5.2 Hz), 7.04–7.06 (2H, d, J=8.8 Hz), 7.15–7.20 (2H, m), 7.44–7.48 (2H, m), 7.70–7.77 (4H, m), 7.99–8.02 (2H, m). ESI-MS m/z: 476 $[M+Na]^+$.

2-(4-(4-Chlorobenzoyl)phenoxy)-2-methyl-*N*-(2-oxo-2-phenylethyl)propanamide (**22f**): Yield 89%, mp 141.2–143.3°C. ^{1}H-NMR (400 MHz, $CDCl_3$) δ: 1.66 (6H, s), 4.79–4.80 (2H, d, J=4.8 Hz), 7.04–7.07 (2H, m), 7.44–7.52 (5H, m), 7.61–7.64 (1H, m), 7.71–7.77 (4H, m), 7.96–7.98 (2H, m). ESI-MS m/z: 436 $[M+H]^+$.

2-(4-(4-Chlorobenzoyl)phenoxy)-2-methyl-*N*-(2-oxo-2-(*p*-tolyl)ethyl)propanamide (**22g**): Yield 83%, mp 124.0–124.3°C. ^{1}H-NMR (400 MHz, $CDCl_3$) δ: 1.65 (6H, s), 2.42 (3H, s), 4.75–4.76 (2H, d, J=4.4 Hz), 7.03–7.05 (2H, d, J=8.0 Hz), 7.25–7.30 (2H, m), 7.43–7.45 (2H, d, J=8.4 Hz), 7.51 (1H, s), 7.70–7.76 (4H, m), 7.85–7.87 (2H, m). ESI-MS m/z: 472 $[M+Na]^+$.

2-(4-(4-Chlorobenzoyl)phenoxy)-2-methyl-*N*-(2-(4-(methylthio)phenyl)-2-oxoethyl)propanamide (**22h**): Yield 89%, mp 113.9–114.6°C. ^{1}H-NMR (400 MHz, $CDCl_3$) δ: 1.69 (6H, s), 2.56 (3H, s), 4.77–4.78 (2H, d, J=4.4 Hz), 7.07–7.09 (2H, d, J=8.8 Hz), 7.32–7.34 (2H, d, J=8.0 Hz), 7.46–7.47 (2H, m), 7.54 (1H, s), 7.74–7.80 (4H, m), 7.89–7.91 (2H, d, J=8.8 Hz). ESI-MS m/z: 504 $[M+Na]^+$.

2-(4-(4-Chlorobenzoyl)phenoxy)-*N*-(2-(3-hydroxyphenyl)-2-oxoethyl)-2-methylpropanamide (**22i**): Yield 69%, mp 168.1–172.3°C. ^{1}H-NMR (400 MHz, $CDCl_3$) δ: 1.53 (6H, s), 3.26 (2H, s), 7.00–7.01 (4H, m), 7.24 (1H, s), 7.51 (1H, s), 7.59–7.62 (4H, m), 7.70–7.73 (4H, m). ESI-MS m/z: 474 $[M+Na]^+$.

General Procedure for the Synthesis of 26[34–36] DMAP (2.0 mmol) and EDCI·HCl (40.0 mmol) were added to a solution of 1-(*tert*-butoxycarbonyl) piperazine **23** (20.0 mmol) and carboxylic acid **14d** (20.0 mmol) in CH_2Cl_2 (125 mL). The reaction mixture was stirred at room temperature for 12 h and then washed with dilute HCl and water. The organic layer was dried over $MgSO_4$, filtered, and the filtrate concentrated *in vacuo* to provide **24**. Compound **24** (2.0 mmol) was dissolved in THF (10 mL), TFA (1 mL) was added, and the resulting mixture shaken at room temperature for 24 h. The reaction mixture was concentrated at reduced pressure and basified with NaOH solution (until pH 10), extracted with CH_2Cl_2, dried over $MgSO_4$, filtered, and evaporated at reduced pressure, and then the residue was purified by chromatography to afford **25**. K_2CO_3 (4.0 mmol) and **11** (2.0 mmol) were added to a solution of **25** (2.0 mmol) in THF (10 mL), and the reaction mixture was stirred at room temperature for 12 h, filtered, and evaporated at reduced pressure. The residue was then purified by chromatography to afford target compound **26**.

2-(4-(4-Chlorobenzoyl)phenoxy)-1-(4-(2-(4-hydroxyphenyl)-2-oxoethyl)piperazin-1-yl)-2-methylpropan-1-one (**26**): Yield 37%, mp 225.6–228.3°C. ^{1}H-NMR (400 MHz, DMSO-d_6) δ: 1.61 (6H, s), 2.12 (2H, s), 2.39 (2H, s), 3.51–3.68 (6H, t), 6.78–6.80 (2H, d), 6.91–6.94 (2H, d), 7.58–7.61 (2H, d), 7.71–7.81 (6H, m), 10.36 (1H, s). ESI-MS m/z: 521 $[M+H]^+$.

Biology Materials HEK293 cells were purchased from

the ATCC (Manassas, VA, U.S.A.). Dulbecco's modified Eagle's medium (DMEM), fetal bovine serum (FBS), ethylenediaminetetraacetic acid (EDTA), phosphate buffered saline (PBS), and OPTI MEM I were purchased from Invitrogen (Carlsbad, CA, U.S.A.). TO901317 and clotrimazole were purchased from Sigma-Aldrich (St. Louis, MO, U.S.A.). pBind-LXRα and pBind-LXRβ and were constructed by Chempartner (Shanghai, P.R. China). Fugene HD Transfection Reagent, pG5Luc plasmid, and the Dual Luciferase Reporter Assay System were purchased from Promega (Madison, WI, U.S.A.).

LXRα(β)/pG5Luc Dual Luciferase Reporter Assay Prior to transfection, HEK293 cells were maintained in DMEM supplemented with 10% FBS in regular tissue culture flasks. The host cells were plated in a 96-well tissue culture plate at a density of 5×10^{-4} cells per well. The transfection mixture contained 25 ng of pBind-LXRα (or pBind-LXRβ) and 25 ng of pG5Luc using 0.15 μL of FuGENE HD transfection reagent per well. Twenty-four hours posttransfection, the transfection medium was removed before 1000 nM of TO901317 and various concentrations of test chemicals dissolved in medium were added for the measurement of antagonistic activity. After treatment with test chemicals for 24 h, the cells were harvested and analyzed immediately using a 96-well plate (Shanghai Bioleaf Biotech Co., Ltd., Shanghai, P.R. China) luminometer. The amounts of firefly luciferase and renilla luciferase were measured with the Dual Luciferase Reporter Assay System kit (Progema) following the manufacturer's instructions. The value of luciferase for each lysate was normalized to the renilla luciferase activity. The percentage of inhibition was calculated using the following formula:

$$\%\ \text{Inhibition} = \left[\frac{1000\ \text{nM TO901317 (firefly/renilla)} - \text{chemical (firefly/renilla)}}{1000\ \text{nM TO901317 (firefly/renilla)} - \text{DMSO (firefly/renilla)}}\right] \times 100\%$$

The IC_{50} values and curve fitting analyses were calculated with a Graphpad prism 5.

Molecular Docking Molecular docking was performed using the program eHiTS v12 from SimBioSys Inc. (Toronto, Canada).[38,39] eHiTS is an exhaustive flexible docking algorithm with a scoring function which incorporates both empirical and knowledge-based features. Open Babel (http://openbabel.org) was used for manipulating the ligand chemical format and acquiring its 3D structure. PyMol (http://www.pymol.org/) was used for visual inspection of the results and the graphical representations.

The crystal structures of LXRα in a complex with the inhibitor GW3965 (PDB entry 3IPQ) and LXRβ with the inhibitor G58 (PDB entry 3L0E) in the Protein Data Bank was selected for the docking study. The eHiTS software package was used for flexible docking. Active site detection was carried out using the "−complex" parameter. The program automatically detected the ligand in the complex and selected the part of the target protein within a 7-Å margin around the ligand as the active site. The compound was then docked into the active site using the highest accuracy mode of docking ("−accuracy" parameter set to 6). The scoring was according to the eHiTS_Score that is included in the eHiTS software package. We selected the compound with the best score and estimated the detailed binding patterns.

Acknowledgments This work was supported by New Drug Innovation 2009X09313-006 from the Ministry of Science and Technology of P.R. China. The authors are thankful to Shanghai ChemPartner Co., Ltd. and Shanghai PharmoGo Co., Ltd. for experimental assistance.

Conflict of Interest The authors declare no conflict of interest.

References

1) Pascual-García M., Valledor A. F., *Arch. Immunol. Ther. Exp.*, **60**, 235–249 (2012).
2) Mangelsdorf D. J., Thummel C., Beato M., Herrlich P., Schütz G., Umesono K., Blumberg B., Kastner P., Mark M., Chambon P., Evans R. M., *Cell*, **83**, 835–839 (1995).
3) Janowski B. A., Grogan M. J., Jones S. A., Wisely G. B., Kliewer S. A., Corey E. J., Mangelsdorf D. J., *Proc. Natl. Acad. Sci. U.S.A.*, **96**, 266–271 (1999).
4) Yang C., McDonald J. G., Patel A., Zhang Y., Umetani M., Xu F., Westover E. J., Covey D. F., Mangelsdorf D. J., Cohen J. C., Hobbs H. H., *J. Biol. Chem.*, **281**, 27816–27826 (2006).
5) Wójcicka G., Jamroz W. A., Horoszewicz K., Bełtowski J., *Postepy Hig. Med. Dosw.*, **61**, 736–739 (2007).
6) Porkkala-Sarataho E., Salonen J. T., Nyyssonen K., Kaikkonen J., Salonen R., Ristonmaa U., Diczfalusy U., Brigelius-Flohe R., Loft S., Poulsen H. E., *Arterioscler. Thromb. Vasc. Biol.*, **20**, 2087–2093 (2000).
7) Zhao C., Dahlman-Wright K., *J. Endocrinol.*, **204**, 233–240 (2010).
8) Faulds M. H., Zhao C., Dahlman-Wright K., *Curr. Opin. Pharmacol.*, **10**, 692–697 (2010).
9) Huang C., *J. Intern. Med.*, **12**, 76–85 (2014).
10) Viennois E., Mouzat K., Dufour J., Morel L., Lobaccaro J. M., Baron S., *Mol. Cell. Endocrinol.*, **351**, 129–141 (2012).
11) Schultz J. R., Tu H., Luk A., Repa J. J., Medina J. C., Li L., Schwendner S., Wang S., Thoolen M., Mangelsdorf D. J., Lustig K. D., Shan B., *Genes Dev.*, **14**, 2831–2838 (2000).
12) Mitro N., Mak P. A., Vargas L., Godio C., Hampton E., Molteni V., Kreusch A., Saez E., *Nature* (London), **445**, 219–223 (2007).
13) Dodo K., Aoyama A., Noguchi-Yachide T., Makishima M., Miyachi H., Hashimoto Y., *Bioorg. Med. Chem.*, **16**, 4272–4285 (2008).
14) Hong C., Tontonoz P., *Nat. Rev. Drug Discov.*, **13**, 433–444 (2014).
15) Calkin A. C., Tontonoz P., *Nat. Rev. Mol. Cell Biol.*, **13**, 213–224 (2012).
16) Collins J. L., Fivush A. M., Watson M. A., Galardi C. M., Lewis M. C., Moore L. B., Parks D. J., Wilson J. G., Tippin T. K., Binz J. G., Plunket K. D., Morgan D. G., Beaudet E. J., Whitney K. D., Kliewer S. A., Willson T. M., *J. Med. Chem.*, **45**, 1963–1966 (2002).
17) Shenoy S. D., Spencer T. A., Mercer-Haines N. A., Alipour M., Gargano M. D., Runge-Morris M., Kocarek T. A., *Drug Metab. Dispos.*, **32**, 66–71 (2004).
18) Houck K. A., Borchert K. M., Hepler C. D., Thomas J. S., Bramlett K. S., Michael L. F., Burris T. P., *Mol. Genet. Metab.*, **83**, 184–187 (2004).
19) Katz A., Udata C., Ott E., Hickey L., Burczynski M. E., Burghart P., Vesterqvist O., Meng X., *J. Clin. Pharmacol.*, **49**, 643–649 (2009).
20) Quinet E. M., Basso M. D., Halpern A. R., Yates D. W., Steffan R. J., Clerin V., Resmini C., Keith J. C., Berrodin T. J., Feingold I., Zhong W., Hartman H. B., Evans M. J., Gardell S. J., DiBlasio-Smith E., Mounts W. M., LaVallie E. R., Wrobel J., Nambi P., Vlasuk G. P., *J. Lipid Res.*, **50**, 2358–2370 (2009).
21) Loren J., Huang Z., Laffitte B. A., Molteni V., *Expert Opin. Ther. Pat.*, **23**, 1317–1335 (2013).
22) Tamehiro N., Sato Y., Suzuki T., Hashimoto T., Asakawa Y., Yokoyama S., Kawanishi T., Ohno Y., Inoue K., Nagao T., Nishimaki-

Mogami T., *FEBS Lett.*, **579**, 5299–5304 (2005).
23) Goldwasser J., Cohen P. Y., Yang E., Balaguer P., Yarmush M. L., Nahmias Y., *PLoS ONE*, **5**, e12399 (2010).
24) González-Granillo M., Steffensen K. R., Granados O., Torres N., Korach-André M., Ortíz V., Aguilar-Salinas C., Jakobsson T., Díaz-Villaseñor A., Loza-Valdes A., Hernandez-Pando R., Gustafsson J. Å., Tovar A. R., *Diabetologia*, **55**, 2469–2478 (2012).
25) Hoang M. H., Jia Y., Jun H. J., Lee J. H., Hwang K. Y., Choi D. W., Um S. J., Lee B. Y., You S. G., Lee S. J., *Mol. Nutr. Food Res.*, **56**, 900–911 (2012).
26) Sheng X., Wang M., Lu M., Xi B., Sheng H., Zang Y. Q., *Am. J. Physiol. Endocrinol. Metab.*, **300**, E886–E893 (2011).
27) Griffett K., Solt L. A., El-Gendy B. E.-D. M., Kamenecka T. M., Burris T. P., *ACS Chem. Biol.*, **8**, 559–567 (2013).
28) Aoyama A., Endo-Umeda K., Kishida K., Ohgane K., Noguchi-Yachide T., Aoyama H., Ishikawa M., Miyachi H., Makishima M., Hashimoto Y., *J. Med. Chem.*, **55**, 7360–7377 (2012).
29) Menke J. G., Macnaul N. S., Hayes N. S., Baffic J., Chao Y. S., Elbrecht A., Kelly L. J., Lam M. H., Schmidt A., Sahoo S., Wang J., Wright S. D., Xin P., Zhou G., Moller D. E., Sparrow C. P., *Endocrinology*, **143**, 2548–2558 (2002).
30) Temple C. Jr., Wheeler G. P., Elliott R. D., Rose J. D., Kussner C. L., Comber R. N., Montgomery J. A., *J. Med. Chem.*, **25**, 1045–1050 (1982).
31) Breslin H. J., Diamond C. J., Kavash R. W., Cai C., Dyatkin A. B., Miskowski T. A., Zhang S. P., Wade P. R., Hornby P. J., He W., *Bioorg. Med. Chem. Lett.*, **22**, 4869–4872 (2012).
32) Le G., Vandegraaff N., Rhodes D. I., Jones E. D., Coates J. A., Thienthong N., Winfield L. J., Lu L., Li X., Yu C., Feng X., Deadman J. J., *Bioorg. Med. Chem. Lett.*, **20**, 5909–5912 (2010).
33) Chen J., Liu D., Butt N., Li C., Fan D., Liu Y., Zhang W., *Angew. Chem. Int. Ed. Engl.*, **52**, 11632–11636 (2013).
34) Rouf A., Aga M. A., Kumar B., Taneja S. C., *Tetrahedron Lett.*, **54**, 6420–6422 (2013).
35) Kim M. K., Lee H. S., Kim S., Cho S. Y., Roth B. L., Chong Y., Choo H., *Bioorg. Med. Chem.*, **20**, 1139–1148 (2012).
36) Khan M. F., Kumar P., Pandey J., Srivastava A. K., Tamrakar A. K., Maurya R., *Bioorg. Med. Chem. Lett.*, **22**, 4636–4639 (2012).
37) https://www.eurofinspanlabs.com/Catalog/Products/ProductDetails.aspx?prodId=uU1gNlSuSeY%3d&path=7,169&leaf=7,169&track=Add%2f2%2fTarget+Class%2fNuclear+Receptor#.
38) Zsoldos Z., Reid D., Simon A., Sadjad B. S., Johnson A. P., *Curr. Protein Pept. Sci.*, **7**, 421–435 (2006).
39) Zsoldos Z., Reid D., Simon A., Sadjad B. S., Johnson A. P., *J. Mol. Graph. Model.*, **26**, 198–212 (2007).